行政院國家科學委員會專題研究計畫 成果報告

提升奈米級零價鐵在地下水層孔隙間移動性之研究
研究成果報告(精簡版)

計 畫 類 別 ：個別型
計 畫 編 號 ：NSC 97-2221-E-041-012-
執 行 期 間 ：97 年 08 月 01 日至 98 年 07 月 31 日
執 行 單 位 ：嘉南藥理科技大學環境工程與科學系（所）

計 畫 主 持 人 ：蔡利局

計畫參與人員：碩士班研究生-兼任助理人員：謝偉智

報 告 附 件 ：出席國際會議研究心得報告及發表論文

處 理 方 式 ：本計畫可公開查詢

中 華 民 國 98 年 10 月 28 日

行政院國家科學委員會補助專題研究計畫 ■ 成 果 報 告 □期中進度報告

提升奈米級零價鐵在地下水層孔隙間移動性之研究

計畫類別：■ 個別型計畫　　□ 整合型計畫
計畫編號：NSC　97-2221-E-041 -012 -
執行期間：97 年 8 月 1 日至　　98 年 7 月 31 日

計畫主持人：蔡利局
共同主持人：
計畫參與人員： 張文奇、謝偉智

成果報告類型(依經費核定清單規定繳交)：■精簡報告　□完整報告

本成果報告包括以下應繳交之附件：
□赴國外出差或研習心得報告一份
□赴大陸地區出差或研習心得報告一份
■出席國際學術會議心得報告及發表之論文各一份
□國際合作研究計畫國外研究報告書一份

處理方式：除產學合作研究計畫、提升產業技術及人才培育研究計畫、列管計畫及下列情形者外，得立即公開查詢
□涉及專利或其他智慧財產權，□一年□二年後可公開查詢

執行單位：嘉南藥理科技大學

中　華　民　國　98 年 10 月 30 日

中文摘要、

經十幾年之實驗室研究及實場應用，已證明毫米級、微米級、尤其是奈米級顆粒大小零價鐵可應用於還原去除地下水中含氯有機污染物、硝酸根離子及鉛、鉻等無機污染物，且為極少數對環境友善之還原去除地下水中污染物藥劑。現行零價鐵實場應用方式主要藉由半滲透反應牆(PRB)讓地下水污染物自行移入反應牆中被分解或以現地注入泥漿狀零價鐵方式處理污染物，但零價鐵在地下水孔隙間移動距離有限只能處理注入點週遭有限範圍之地下水中污染物。奈米級零價鐵效能高於粒狀及微米級零價鐵主要原因為擁有較大之比表面積。但奈米級零價鐵現地應用於地下水污染場址時，易因凡得瓦爾力呈現團狀凝聚進而阻塞、吸附或吸收在地下含水層中土壤顆粒，縮短奈米級零價鐵在地層孔隙移動到污染團之距離。為達成現地處理地下水中污染物目標需增加奈米級零價鐵注入井數量，導致提高整治工程費用及操作不便性。如能使用分散劑(Dispersant)使奈米級零價鐵在地下水中維持奈米級膠體穩定分散性，減少凝聚性及被土壤顆粒吸附之數量，增加奈米級零價鐵隨地下水移動距離，將可提高奈米級零價鐵之現地處理工程應用性。本研究探討幾種常見分散劑(SDBS、SDS、CMC、PAA、PEI、PVG、alginic acid、sodium alginate、gelatine 等)，在各種濃度及 pH 值影響奈米級零價鐵合成粒徑；並探討奈米級零價鐵在模擬含水飽和管柱空隙中移動性受分散劑之影響。實驗結果發現 CMC、PAA、尤其是混合型 CMC+PAA 分散劑有穩定分散零價鐵顆粒效果，使合成零價鐵分別達到奈米級尺寸 12、31、及 19.1 nm，並且提高零價鐵穿透砂層孔隙效能分別達 282、219、及 284 倍。

關鍵詞：零價鐵、分散劑、移動性、砂管柱

英文摘要、

Zero valent iron (ZVI) sized with millimeter, micrometer, particularly nanoscale has been used for groundwater remediation, polluted with halogenated organic compounds, lead (II), chromium(VI) and nitrates through lab studies and in in-situ application. The most frequent applications of ZVI are packed at permeable reactive barrier (PRB) or directly injected into contaminated hot spots of sites. The contaminants in groundwater flew into the PRB and reduced with ZNI. The ZNI slurry can treat contaminants around the injection point and migrated only small distance in the porosity of groundwater layer. The nanoscale ZVI having larger specific surface area made higher decontamination efficiency than millimeter and micrometer-sized ZVI. However, higher reactivity of NZNI did not have enough reason to select as in-situ remediation chemical agent. The reduction of migration distance of ZVI caused by the aggregation, absorption and adsorption of ZNI to aquifer materials in saturated porous media limited the in-situ application of ZVI. If the migration distance of ZVI was enhanced with dispersant, the acceptance and convenience of ZVI will be improved in in-situ remediation technology. The general dispersants with varied concentration and pH were selected to test the dispersion of aqueous ZVI, including SDBS、SDS、CMC、PAA、PEI、PVG、alginic acid、sodium alginate、and gelatin etc..The migration of nanoscale zero valent iron (NZVI) affected with dispersants in sand column also was discussed. According to the experimental results, CMC, PAA, and mixed dispersant of CMC and PAA could disperse and stabilize the ZVI, and reduced the synthesized NZVI particles sizes to 12,31,and 19.1 nm. Comparison with ZVI product without addition of dispersant, the migration efficiency

of ZVI acted by dispersant through water saturated sand column increased 282、219、and 284 times for CMC,PAA, and CMC+PAA, respectively.

Keywords: Zero valent iron, Dispersant, Migration, sand column.

1.前言、

奈米級零價鐵能快速整治地下水中污染物，但在含水飽和孔隙間移動性仍受限制。如能藉由添加陰離子型界面活性劑或分散劑，保持奈米級零價鐵在地下含水層孔隙間維持奈米級顆粒態分散穩定狀態，將可提升奈米級零價鐵在地下水層孔隙間移動效能，則可更加擴展奈米級零價鐵在野外場址污染物整治之實用性，特別是受污染場址環境地形受限於地形、建築物廠房地基、及生產線不能停工等限制條件，致無法以鑿井、開挖透水性反應牆進行整治、或污染團深度超過 20 公尺之地下含水層、或工廠生產線下方等。奈米級零價鐵在地下含水層孔隙間之分散穩定度及移動能力變成限制奈米級零價鐵是否可被廣泛使用之最重要決定因素[1-3]。

2.研究目的、

許多可使奈米級零價鐵懸浮液維持分散穩定性之陰、陽離子型界面活性分散劑、無機性分散劑、聚合物分散劑曾被研究發表過[1, 4, 5, 6, 7, 8, 9, 10]，且亦被證實在燒杯中可達到分散穩定膠體之目標，但如注入沙、泥土構成之孔隙間則膠體是否仍能維持分散穩定性，及隨地下水流之流動性則缺乏研究證明。因此本研究主要目標為找到使奈米級零價鐵穩定分散且能在模擬之地下水孔隙間快速移動之各種陰離子型界面活性劑或分散劑。

探討奈米級零價鐵懸浮液分散穩定性是否受各種陰離子型界面活性劑或分散劑種類、濃度、混合型分散劑之影響，並測試加入分散劑之奈米級零價鐵懸浮液在人工土壤管柱含水層孔隙間移動性。

3.文獻回顧、

奈米級零價鐵(零價鐵)於 1996 年首次被應用於整治受污染場址及處理有害廢棄物[11]。十幾年來里海大學(Lehigh University)張博士(Wei-xian Zhang)研究團隊嘗試應用零價鐵處理各種污染物之研究最為完整，張博士團隊將研究結果發表約數十幾篇文章於國際著名期刊[1-3, 12-20, 21-22]。其主要之創新成就有：奈米級零價鐵合成技術、奈米級零價鐵顆粒表面特性修飾改良及提升野外實場整治應用效能等。目前對奈米級零價鐵(零價鐵)之研究已證實奈米級零價鐵(零價鐵)為經濟便宜有效、對環境友善、較無不良附產物產生，適宜應用於地下水體中污染物整治去除的整治技術，研究結果已證明可將許多環境汙染物還原轉化成無害物，如將含氯有機溶劑[12，17，22](*ter*-butyl ether, Hexachlorobenzene, tetra-chlorobenzene, tri-chlorobenzene, dichlorobenzene, tetrachloroethene, trichloroethene, dichloroethene, vinyl chloride etc.)；有機氯農藥[13]；多氯聯苯(Polychlorinated biphenyls)[17]；和有機染料藉由還原去氯(Dechlorination)轉化作用生成毒性較低且微生物容易分解之有機物；將六價鉻[2，23]還原轉化成 $Cr(OH)_3$、$Cr_xFe_{1-x}(OH)_3$ 不易移動之沉澱物；還原及吸附二價鉛[23]及二價鎳[15, 18]；將硝酸根還原轉化生成 NH_4^+[24]等。美國對於零價鐵實場整治應用實例有將粘土混合之零價鐵泥漿和受四氯化碳污染場址，進行現地土壤混合成直徑 8 英呎之混合泥柱，整治後可將四氯化碳濃度由 4000mg/kg 降至 0.21mg/kg[25]，實際場址如維吉尼亞州之 Martinsville 尼龍工廠、北卡羅來納州之 Camp Lejeune 乾洗工廠及田納西州 Arnold 空軍基地廢棄物最終處置場。另一常見之奈米級零價鐵現地整治技術為將奈米級零價鐵放在透水性反應牆中，地下水中污染物流經透水性反應牆，即可被具有大表面積之奈米級零價鐵還原去除。最理想之奈米級零價鐵應用技術為現地注入奈米級零價鐵至地下污染團，讓奈米級零價鐵隨地下水流移動至污染團

位置，但主要應用限制為奈米級零價會因凡得瓦爾力相互吸引凝聚、膠凝使粒徑變大、發生沉澱作用或因過濾作用而受到地下飽和含水孔隙阻滯，限制移動傳輸距離[26]。

零價鐵及 Fe_3O_4(Magnetite)皆為具磁性物質。外覆有磁性鐵氧化物 Fe_3O_4(Magnetite)之奈米級零價鐵顆粒間存在之磁性吸引力大於外覆低磁性鐵氧化物 α-Fe_2O_3(Hematite)之奈米級零價鐵顆粒，因此更易失去膠體穩定性，凝聚形成較大尺吋之奈米級零價鐵團粒[27]。因磁性吸引力凝聚之奈米級零價鐵通常會形成條鏈狀團粒。奈米級零價鐵具有大比表面積及伴隨而來和污染物間之快速接觸反應速度，使其適宜應用於受污染場址之整治處理。但近年來之實場應用發現奈米級零價鐵在飽和含水孔隙間移動性只有幾公分[4]，推測奈米級零價鐵在孔隙間移動距離短之原因可能有：(1)流經地下水層孔隙物質時奈米級零價鐵被過濾吸附、(2)奈米級零價鐵之凝聚(Aggregation)沉澱及膠凝作用(gelation)成網狀結構導致奈米級零價鐵尺吋增大而阻塞地下水層孔隙、(3)只有粒徑小於幾百 nm 之膠體才具有擴散作用。奈米級零價鐵必須能以細小顆粒均勻分散於地下水中且不易被多孔隙材質吸附吸收，才能藉擴散作用及流動性流經飽和含水孔隙到達下游污染團發揮其快速反應之特性。

可改變水中膠體顆粒表面電荷使膠體顆粒保持分散性之分散劑，可分成有機界面活性分散劑及無機界面活性分散劑二大類[6]。已有研究報告[5]提出可應用於使奈米級磁性鐵氧化物物質 Fe_3O_4(Magnetite)顆粒均勻分散之有機性分散劑有油酸(Oleic acid)[7]、Phospholipids[8]、Polyvinylpyrrolidone(PVP)、polyacrylamide(PAA)、(Poly-methcacrylic acids, PMAA)[10]、poly(ethylene glycol)(PEG)、poly(vinyl alcohol)(PVA)、poly(ethylene oxide)(PEO)、sodium dodecyl sulfate (SDS)[9]、Aerosol MA-1[9]、Poly-styrenesulfonic acid[5]、Poly-vinylsulfonic acid[5]、Poly-cacrylic acids, (PAA)[4, 10]、poly(ethylene imine)(PEI)以及 Polyvinyl alcohol-co-vinyl acetate-co-itaconic acid (PV3A)[1]等。無機性分散劑有 Polyphosphate[6]等。

有機性界面活性分散劑可使水中奈米級膠體顆粒維持分散狀態[1, 4]，存在顆粒間之排斥力作用機制可歸納成三種：(1)被有機性界面活性分散劑吸附之膠體顆粒如帶有正或負電荷，顆粒間將存在靜電排斥力(electrostatic interaction force)，(2) 被吸附之有機性界面活性分散劑如有一端自顆粒膠體表面延伸進入溶液中，將出現立體排斥力(repulsive steric force)，(3) 靜電排斥力和立體排斥力形成之共同作用力(electrosteric interaction force)。不同於有機性界面活性分散劑使膠體穩定機制，無機性界面活性分散劑因分子量小，通常不能於膠體間構成立體排斥力(repulsive steric force)，同時無機性界面活性分散劑不但會水解於水溶液中同時可能會和膠體顆粒起化學作用[6]。

膠體穩定性來自於膠体顆粒間抗互相凝聚作用之位能障礙(Energy barrier)值高。根據 DLVO (Deryaguin-Landau-Verywey-Overbeek)理論[27]存在膠体顆粒間淨作用力為凡德瓦爾吸引力和靜電雙層排斥力總和，並受顆粒大小、Hamaker 常數、顆粒表面電位、及溶液離子強度之影響。

膠體顆粒表面帶不相同電荷將相互吸引失去穩定性而凝聚增加顆粒尺寸形成膠羽，帶相同電荷膠體顆粒將互相排斥維持穩定之懸浮液[4]。膠體顆粒表面之 ζ potential 越趨向於零，膠體間之凡德瓦爾力越易超過靜電荷排斥力使膠體穩定性變差，越易發生凝聚(Flocculation)及沉澱作用(Sedimentation)。為維持膠體穩定性，ζ potential 應大於 30 mV 或小於－30 mV[20]。地下含水層孔隙由各種不同粒徑之土壤顆粒堆疊而成，不同大小之土壤顆粒因表面官能基而常帶負電荷，如能添加陰、陽離子型界面活性劑或分散劑保持奈米級零價鐵和含水層孔隙間顆粒具有相同之電荷，且維持 ζ potential 大於 30 mV 或小於－30 mV，可防止奈米級零價鐵被含水層孔隙間顆粒吸附，使奈米級零價鐵能穩定分散在含水層孔隙間，增加自由移動距離而不被土壤顆粒吸附。因此水溶液中顆粒表面電荷高於離子強度，顆粒間之淨作用力為排斥力且可形成低滯度穩定懸浮液。相反的，顆粒表

面電荷低於離子強度則奈米級零價鐵將會發生凝聚現象。只依賴控制 pH 值變化來達成穩定性懸浮液是不足的。通常最有效方法為加入化學性穩定分散劑來分散及穩定細小微粒，穩定分散劑可為聚合物及界面活性劑，它會吸附於顆粒表面、改變表面電荷、和靜電吸引力。最主要穩定分散懸浮液之力量為顆粒表面電荷形成之靜電排斥力，其他還有立體排斥力、靜電立體斥力[28]。存在顆粒間維持膠體穩定性之能量包括凡德瓦爾吸引力、表面電荷排斥力、顆粒表面吸附聚合電解質生成之立體排斥力、懸浮液中未吸附電解質形成之位能[5, 29]。

4.研究方法與步驟、

4.1 實驗材料：

本研究所使用之化學藥劑皆為試藥級以上藥品，如 Merck、Fluka 或 Aldrich 公司產品。以二次蒸餾水配製之試藥貯備液於使用前放置於 4℃冷藏。

4.2 分析方法

4.2.1 紫外光-可見光分光光度計(UV/visible spectroscopy)：

將含有奈米級微粒水樣置於 1 公分光路徑石英比色槽，使用紫外光-可見光分光光度計(JASCO V-630，JASCO Inc., Japan)於 220－900 nm 波長範圍進行吸光度掃描，掃描解析度為 0.5 nm。

4.2.2 動態光散射粒徑分析儀(Dynamic light scattering, DLS)：

測量水樣中奈米級微粒尺寸大小及分布，採用動態光散射粒徑分析儀(N5 Submicron Particle Size Analyzer, Beckman coulter inc., USA). 光源為 25 mW， He-Ne 雷射光源，波長設定為 632.8 nm，散射角度為 90。。

4.2.3 粒徑分析及界達電位分析儀(Particle Size and Zeta Potential Analyzer)：

利用粒子因帶電性於外加電場中的泳動行為所造成之光散射現象轉換成粒子之界達電位，使用之儀器為動態光散射粒徑分析儀及界面電位分析儀(Malvern, Zetasizer NANO ZS)，可量測 1~2000nm 樣品粒子之粒徑分佈及界面電位。

4.2.4 孔隙率(%)：比較滴定管中多孔隙材質飽和含水及乾燥狀態下之重量差異進行計算。

4.2.5 總鐵分析：啡囉琳比色法(Standard Method)

4.2.5.1. 取 50mL 水樣或適量水樣稀釋至 50mL 裝入 125mL 錐形瓶，加入 2mL 濃鹽酸、1mL 羥胺(hydroxylamine)溶液，加入數顆玻璃珠加熱至沸騰，直至體積減少至 15～20mL。樣品中如還有灰燼等不透明物再加入 2mL 濃鹽酸、5mL 水繼續加熱。

4.2.5.2. 冷卻至室溫後，移至 100mL 定量瓶，加入 10mL 醋酸銨緩衝溶液、4mL 菲羅琳指示劑稀釋至刻度，混合均勻靜置 10 分鐘使呈橘紅色，但不可陽光直射，以波長 510nm 分光光度計測吸光值。

4.2.5.3. 標準檢量線製作：

取 0、5、10、20、30、40、50 mL 鐵標準溶液(10 μg Fe/mL)，裝入 125mL 錐形瓶以蒸餾水稀釋至 50mL，加入 2mL 濃鹽酸、1mL 羥胺(hydroxylamine)溶液，移至 100mL 定量瓶。加入 10mL 醋酸銨緩衝溶液、4 mL 菲羅琳指示劑稀釋至刻度，混合均勻靜置 10 分鐘使呈橘紅色，但不可陽光直射，以 0 mL 鐵標準溶液於波長 510nm 分光光度計歸零。測出其他鐵標準溶液吸光值，並繪出其檢量線。(對應吸光值之檢量線鐵含量分別為 0、50、100、200、300、400、500 μg Fe)。

4.2.5.4. 計算：mg Fe/L＝(100Ml 之最終稀釋體積中 Fe 含量(μg))÷(水樣體積(mL))

4.3 各種奈米級零價鐵之製備方法：

4.3.1 未添加分散劑奈米級零價鐵之製備[11]：

秤取 0.9732g $FeCl_3 \cdot 6H_2O$(270.3g/mol)於 1000mL 去離子水中(3.6×10^{-3}M)，置於血清瓶，放入厭氧箱中，通入高純氮氣，並溶解 0.756g $NaBH_4$(37.8g/mol)於 1000mL 去離子水(0.02M)，置

於血清瓶，放入厭氧箱中，通入高純氮氣，經 30 分鐘後達無氧條件。取 100 mL Fe^{3+}溶液於燒杯中，將 100mL BH_4^-溶液於 10 分鐘平均緩慢加入於燒杯中，並以磁石進行均勻攪拌，達兩液體之體積比為 1：1 混合比，(Fe^{3+}和 BH_4^-mol 比為 3.6×10^{-3}：0.02；即 1：5.6)，繼續攪拌至反應溶液中無所氫氣產生為止，得到之黑色固體即為 0.1g/L 之奈米級零價鐵。使用 cupper Grid 採樣置於厭氧之採樣瓶中。

4.3.2 被聚合物分散劑分散穩定之奈米零價鐵之製備方法：

4.3.2.1、CMC(**Carboxymethyl cellulose sodium salt**)

(1)、取 9g Carboxymethyl cellulose sodium salt (M.W. 90000)溶入 1000mL 去離子水中形成 0.0001M CMC stock 溶液，

(2)、秤取 4.8654 g $FeCl_3$ ・ $6H_2O$(270.3g/mol)於 1000mL 去離子水(0.018M Fe^{3+}溶液)。

(3)、取 0.4、0.8、2、3.2、4、16、32、40 及 80 mL 之 0.0001M CMC 溶液置於血清瓶，各別加入 20 mL 之 0.018M Fe^{3+}溶液，加蒸餾水稀釋至 100mL，放入厭氧箱中，通入高純氮氣，並溶解 0.756g $NaBH_4$(37.8g/mol)於 1000mL 去離子水(0.02M BH^{4+}溶液)，置於血清瓶，放入厭氧箱中，通入高純氮氣，經 30 分鐘後達無氧條件。(2×10^{-6}M、4×10^{-6}M、1×10^{-5}M、1.6×10^{-5}M、2×10^{-5}M、8×10^{-5}M、1.6×10^{-4}M、2×10^{-4}M、及 5×10^{-4}M 之 CMC 分散劑)。

(4)、測混合液 pH 值。

(5)、取 100 mL 含各種濃度 CMC 之 3.6×10^{-3}M Fe^{3+}溶液於燒杯中，將 100mL BH^{4-}溶液於 10 分鐘內平均緩慢加入於燒杯中，並以磁石進行均勻攪拌，達兩液體之體積比為 1：1 混合比，(Fe^{3+}和 BH^{4-}mol 比為 3.6×10^{-3}：0.02；即 1：5.6)，，繼續攪拌至反應溶液中無氫氣產生為止，所得之黑色固體即為被各種濃度 CMC 分散之 0.1g/L 奈米級零價鐵。使用 cupper Grid 採樣置於厭氧之採樣瓶中。

(6)、於厭氧箱中將生成之奈米鐵顆粒 200mL，分裝成五瓶，裝入玻璃樣品瓶中，關緊蓋子保持厭氧狀態，自厭氧箱中取出，立即進行 DLS、UV-vis 分析及靜置 3、5、10、15 天後再進行 DLS、UV-vis 分析。

(7)、測混合液 pH 值。

4.3.2.2、PEI(poly(ethylene imine))：取 5g poly(ethylene imine) (M.W. 50,000)溶入 1000mL 去離子水中形成 0.0001M PEI stock 溶液，其餘操作步驟同上 2-1。

4.3.2.3、Alginic acid：取 5g Alginic acid 溶入 100mL 去離子水中形成 5% Alginic acid stock 溶液，其餘操作步驟同上 2-1。

4.3.2.4、Sodium alginate：取 5g Sodium alginate 溶入 100mL 去離子水中形成 5% Sodium alginate stock 溶液，其餘操作步驟同上 2-1。

4.3.2.5、PAA(Poly(acrylic acid)：取 5g PAA 原液溶入 100mL 去離子水中形成 3.15% PAA stock 溶液，其餘操作步驟同上 2-1。

4.3.2.6、PEG(Polyethylene glycol)：取 1.5g Polyethylene glycol (M.W. 1500) 溶入 100mL 去離子水中形成 0.01M PEG stock 溶液，其餘操作步驟同上 2-1。

4.3.3. 被陰離子型界面活性劑分散穩定之奈米零價鐵之製備方法：

4.3.3.1、SDS (Sodium Dodecyl sulfate)：取 0.2389g Sodium Dodecyl sulfate (M.W. 238.88) 溶入 100mL 去離子水中形成 0.01M SDS stock 溶液，其餘操作步驟同上 2-1。

4.3.3.2、SDBS(Dodecyl benzenesulfonic acid, sodium salt)：取 0.872g Dodecylbenzene

sulfonic acid, sodium salt 溶入 100mL 去離子水中形成 0.02M SDBS stock 溶液，其餘操作步驟同上 2-1。

4.3.4. 被混合型界面活性劑分散穩定之奈米零價鐵之製備方法：

CMC 混合 PAA：取 9g Carboxymethyl cellulose sodium salt (M.W. 90000)溶入 1000mL 去離子水中形成 0.0001M CMC stock 溶液。取 5g PAA 原液溶入 100mL 去離子水中形成 3.15% PAA stock 溶液，其餘操作步驟同上 2-1。

4.4. pH 影響各種奈米級零價鐵分散劑之分散性：

pH 值影響管柱中構成孔隙材質之等電位點及 ζ 電位，間接造成奈米級零價鐵凝聚、膠化成大顆粒或發生沉澱作用，因此各種經過表面修飾之奈米級零價鐵分散性將受到影響。因此以 1M 硫酸或 1M NaOH 溶液調整各種分散劑分散穩定之奈米級零價鐵懸浮液 pH 值在 4.0～10.0 間，再進行雷射粒徑分析。

4.5. 奈米鐵於含水飽和地下水層孔隙之移動性模擬試驗：

使用內徑 1.2 公分之玻璃材質滴定管出口端裝有鐵氟龍控制閥，為防多孔隙材質砂(sand)自滴定管出口端流失，於鐵氟龍控制閥前填充玻璃纖維棉作為濾層。玻璃滴定管中濾料厚度達 12 公分高，玻璃滴定管中濾料上層置入經各種分散劑分散穩定之奈米鐵懸浮液 20 公分高，量測奈米級零價鐵在各種孔隙體積濾液流出收集後，奈米級零價鐵在管柱孔隙內之穿透深度，於管柱出口端約每隔 2 倍孔隙體積流量，收集濾料出口濾液分析鐵含量。

5.結果與討論、

5.1. 界面活性劑及聚合物分散劑濃度對零價鐵顆粒分散性之影響

未添加分散劑時化學合成之零價鐵平均粒徑約為 1700nm，添加入 2×10^{-5}～8×10^{-4}M 陰離子型界面活性劑 SDBS 未能使零價鐵平均粒徑降低，甚至使零價鐵平均粒徑增加。隨後再增加 SDBS 添加量自 1.6×10^{-3}增至 5×10^{-3} M，零價鐵平均粒徑自 496nm 降低至 302nm(圖 1a)。添加 2×10^{-5}～5×10^{-3}M 陰離子型界面活性劑 SDS，雖可降低合成之零價鐵粒徑，但只可使零價鐵粒徑自 1728nm 降至 893nm(圖 1b)。使用 2×10^{-5}～5×10^{-3}M PEG 聚合物分散劑，皆可使零價鐵合成粒徑降低，並增加分散性，自 1728nm 降至 362nm(圖 1c)。使用 0.0004～0.08% Sodium alginate 皆可使零價鐵粒徑減少，最低粒徑為 111nm(圖 1d)。使用 0.0004～0.04% alginic acid，除 0.0004% alginic acid 外，皆可使零價鐵粒徑減少，最低粒徑為 409nm(圖 1e)。使用 2×10^{-7}～5×10^{-5}M PEI 聚合物分散劑，除 2×10^{-7}及 4×10^{-7}M PEI 外，皆可使零價鐵粒徑降低，增加分散性，自 1728nm 降至 192nm(圖 1f)。使用 0.00126～0.0126% PAA，皆可使零價鐵粒徑降低，增加分散性，自 1728nm 降至 128nm(圖 1g)，每種劑量之 PAA 分散劑皆可使<50 nm 零價鐵顆粒體積比超過 75%以上，相似地，PEI 分散劑亦可使<50 nm 零價鐵顆粒體積比超過 90%以上。2×10^{-7}～5×10^{-5}M CMC 聚合物分散劑對零價鐵顆粒分散性最穩定，且每種濃度都可降低零價鐵顆粒粒徑，最佳 CMC 添加劑量及零價鐵顆粒粒徑為 8×10^{-6}M CMC 及 38.5nm，CMC 分散劑亦可使<50 nm 零價鐵顆粒體積比超過 99%以上(圖 1h)。故 CMC、PAA、PEI 為較佳之零價鐵顆粒分散劑。

5.2. PH 值影響零價鐵顆粒分散劑效果

根據奈米鐵形成之反應方程式，反應溶液中低 pH 值有助於零價鐵形成之速率。圖 2a 中以 2×10^{-5}M CMC 為分散劑，奈米鐵形成前反應液 pH 值 7.0 時，形成之零價鐵平均粒徑約 296nm，<50 nm 零價鐵顆粒體積比為 0%。隨反應液 pH 值降至 6.0 時，零價鐵平均粒徑降低至約 189nm，<50 nm 零價鐵顆粒體積比增為 96.3%。反應液 pH 值降至 5.0 時，零價鐵平均粒徑降至約 145nm，<50 nm 零價鐵顆粒體積比增為 97.3%。奈米鐵形成前反應液 pH 值增至 8.0 時，形成之零價鐵顆粒經雷射粒徑分析測得之平均粒徑稍降為約 289nm，但顆粒物外觀顏色已由黑色轉為紅棕色，代表鐵之氧化物已形成，而非

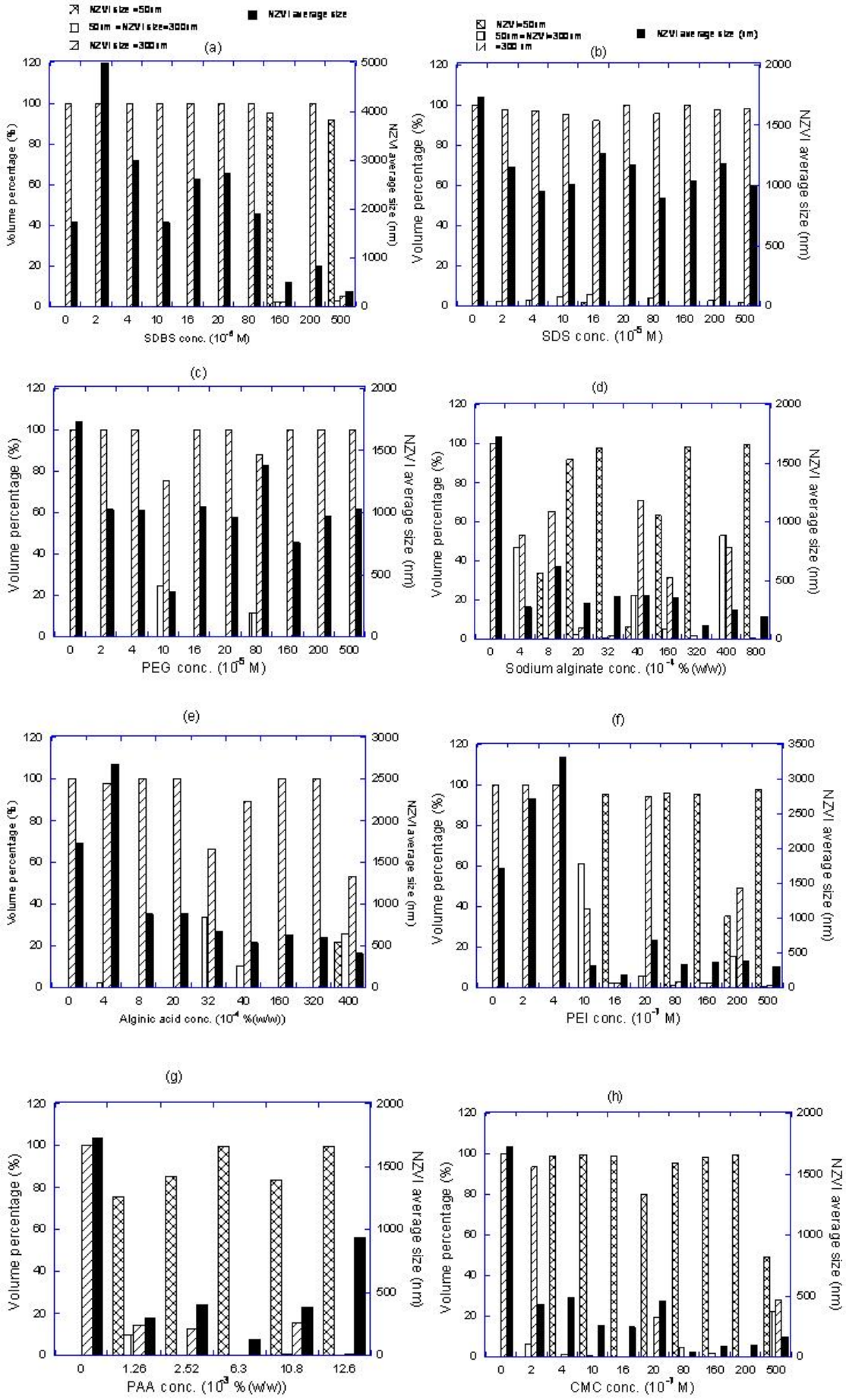

圖 1. 界面活性劑及聚合物分散劑濃度對零價鐵顆粒粒徑分佈之影響

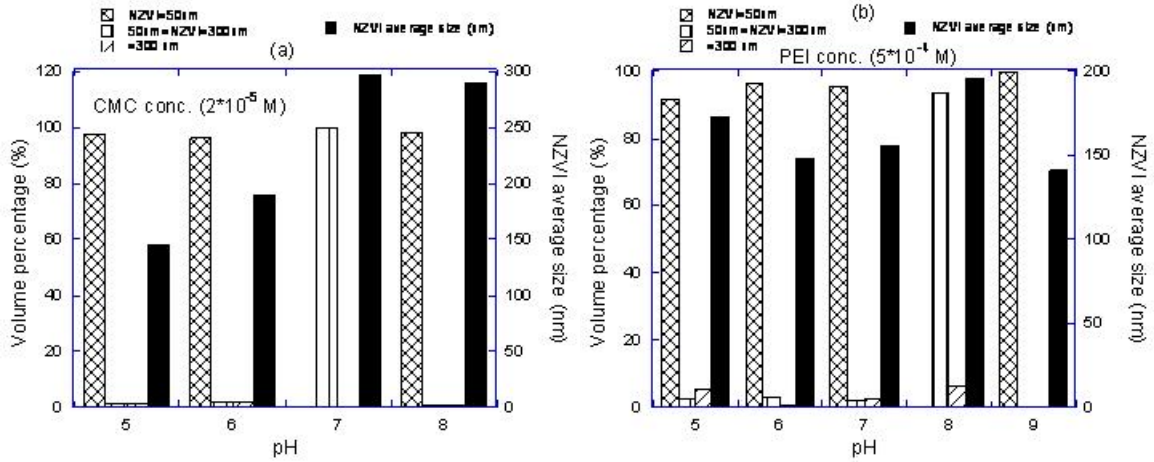

圖 2. PH 值及 CMC、PEI 濃度影響形成零價鐵顆粒粒徑及分佈

單純之零價鐵顆粒。PEI 分散劑最佳幫助零價鐵分散穩定之 pH 值為 6.0，此時零價鐵平均顆粒粒徑增加為 148nm，<50 nm 零價鐵顆粒體積比增為 96.3%；pH 值升高至 7.0 或降低至 5.0 皆使零價鐵平均顆粒粒徑增加為 156 及 173nm，<50 nm 零價鐵顆粒體積比減為 95.3 及 91.9%(圖 2b)。pH 值增加至 8.0 時，合成之顆粒物外觀顏色已由黑色轉為紅棕色，代表鐵之氧化物已漸形成，而非單純之零價鐵顆粒；pH 值增加至 8.0 時，溶液轉為紅棕色鐵氧化物，故顆粒粒徑減少，<50 nm 零價鐵顆粒體積比增加。

5.3. 分散劑對奈米鐵顆粒特性之影響

於表 1 中，添加 0.0063% PAA 於 0.1g/L 鐵(Fe^{3+})溶液中合成之零價鐵顆粒，其界達電位(Zeta potential)為-49.2±1.56 mV。添加 2×10^{-6} M CMC 於 0.1g/L 鐵(Fe^{3+})溶液中合成之零價鐵顆粒界達電位為-36.6±1.57 mV；隨者 CMC 添加濃度增加至 4×10^{-6} M 及 8×10^{-6} M，零價鐵顆粒之界達電位增加至-48.9±1.25 mV 及-46.4±2.18 mV。三種不同 CMC 作用合成之零價鐵顆粒穩定性最佳者為界達電位-48.9±1.25 mV。添加 PAA 混合 CMC 之共用分散劑，隨 CMC 濃度增加零價鐵顆粒降低且界達電位維持在負值(-31.6～-48.6 mV)。Alginic acid 分散劑對零價鐵顆粒分散作用較差，其界達電位只有-3.52±0.16 mV，顆粒粒徑達 1812 nm。相反地，不同濃度 PEI(1×10^{-6}～1.6×10^{-5} M)分散劑可使合成之零價鐵鐵顆粒分散，界達電位為正值，介於 16.2～26.9 mV。

5.4.分散劑對零價鐵通過砂管柱之影響

將合成且未加分散劑之 0.1g Fe/L 零價鐵通過石英砂層管柱，收集約 5 倍孔隙體積濾液，濾液中測得知總鐵含量甚低(約 0.34mg Fe/L)(圖 3a)。加入 0.0063% PAA 於零價鐵合成反應過程，濾液中測得知總鐵含量隨濾液體積增加而增高。流過 4.8 倍孔隙體積濾液中測得總鐵含量 78.4mg Fe/L，與未加分散劑之 0.1g Fe/L 零價鐵通過石英砂層管柱比較，最高達 230 倍穿透性。加入 CMC 於零價鐵合成反應過程，濾液中測得知總鐵含量隨濾液體積增加而增高，先隨添加 CMC 濃度增加而增加(2×10^{-5} M CMC 增加至 8×10^{-5} M CMC)，而後添加至 1.6×10^{-4} M CMC 時，測得濾液中總鐵含量降低，與未加分散劑之 0.1g Fe/L 零價鐵通過石英砂層管柱比較，最高達 282 倍穿透性。同時添加 0.0063% PAA 及 4×10^{-5} M CMC 分散劑合成之零價鐵(圖 3b)，經 5 倍孔隙體積後收集到濾液，測得濾液中總鐵含量最高，零價鐵對管柱之穿透性最佳，與未加分散劑之 0.1g Fe/L 零價鐵通過石英砂層管柱比較，最高達 284 倍穿透性。但初始收集到濾液反而是 0.0063% PAA 及 1.6×10^{-4} M CMC 形成之零價鐵穿透性最佳，符合表 1 所述 PAA 混合 CMC 濃度越高，零價鐵顆粒越小，穿透性越佳。

表 1.各種分散劑對奈米鐵顆粒特性之影響(0.1g Fe/L)

分散劑	濃度 (M or %)	平均粒徑 (r.nm)	吸收峰直徑 (d.nm)	Volume (%)	Zeta potential (mV)
PAA	0.0063%	431.0	924.2	92.8	(-49.2±1.56)
			74.8	7.2	
CMC	2×10^{-6}	555.2	1141.0	97.0	(-36.6±1.57)
			119.3	3.0	
	4×10^{-6}	164.0	417.8	100.0	(-48.9±1.25)
	8×10^{-6}	173.0	813.3	100.0	(-46.4±2.18)
PAA+CMC	0.0063%+2×10^{-6}	348.0	984.3	100.0	(-47.8±1.55)
	0.0063%+4×10^{-6}	174.0	713.4	50.7	(-48.6±0.59)
			73.9	49.3	
	0.0063%+8×10^{-6}	3.7	73.2	0.4	(-31.6±3.22)
			7.2	99.6	
Alginic acid	0.10%	1812.0	2249.0	90.0	(-3.52±0.16)
			188.0	10.0	
PEI	1×10^{-6}	206.0	565.1	71.4	(26.9±0.42)
			54.8	28.6	
	8×10^{-6}	172.0	226.0	98.5	(16.2±0.3)
			103.0	1.5	
	1.6×10^{-5}	279.0	279.0	100.0	(17.6±0.36)

5.5.經分散劑分散之零價鐵通過砂柱濾液後顆粒分佈

經 2×10^{-6} M CMC 分散穩定之 12 nm 奈米鐵顆粒，流經石英砂層管柱過程會發生奈米零價鐵顆粒凝聚現象，使濾出液中零價鐵顆粒增加至 1378 nm。隨著濾出液體積增加，零價鐵顆粒平均粒徑漸減，<50 nm 零價鐵顆粒體積比漸漸增加(圖 4a)。提高 CMC 濃度至 4×10^{-6} M，濾出液中零價鐵顆粒平均粒徑先增加，至濾出液達 2.65 倍孔隙體積時達最小粒徑(74.5nm)，而後隨濾出液體積增加，零價鐵顆粒平均粒徑漸增(圖 4b)。在 2×10^{-6} M CMC 及 0.0063% PAA 共同作用下合成之零價鐵顆粒流經石英砂層管柱，於濾出液中零價鐵顆粒降至 102nm，最低達 19.1nm，但濾出液中總鐵含量仍可達 89 mg Fe/L，比單獨使用 2×10^{-6} M CMC 時，濾出液中總鐵含量只有 46.7 mg Fe/L 更具穿透性。在提高 CMC 至 4×10^{-6} M 及 0.0063% PAA 共同作用，濾出液中零價鐵顆粒降至 58.2nm，最低達 9.7nm，但濾出液中總鐵含量仍可達 89 mg Fe/L，但單獨使用 4×10^{-6} M CMC 時，濾出液中總鐵含量可達 93.8 mg Fe/L(圖 4c, d)。單獨使用 0.0063% PAA 合成之零價鐵顆粒流經石英砂層管柱，於濾出液中零價鐵顆粒降至 573nm，最低達 31nm，但濾出液中總鐵含量仍可達 78 mg Fe/L(圖 4e)。

5.6. 分散劑對零價鐵顆粒分散性之吸光圖譜

0.1g/L 零價鐵合成時，分別加入 4×10^{-6} M CMC、0.0063% PAA、4×10^{-6} M CMC＋0.0063% PAA、0.1% alginic acid、1×10^{-6} M PEI、及 0.08% sodium alginate，零價鐵顆粒懸浮液以 UV-VIS 分光光度計，測量

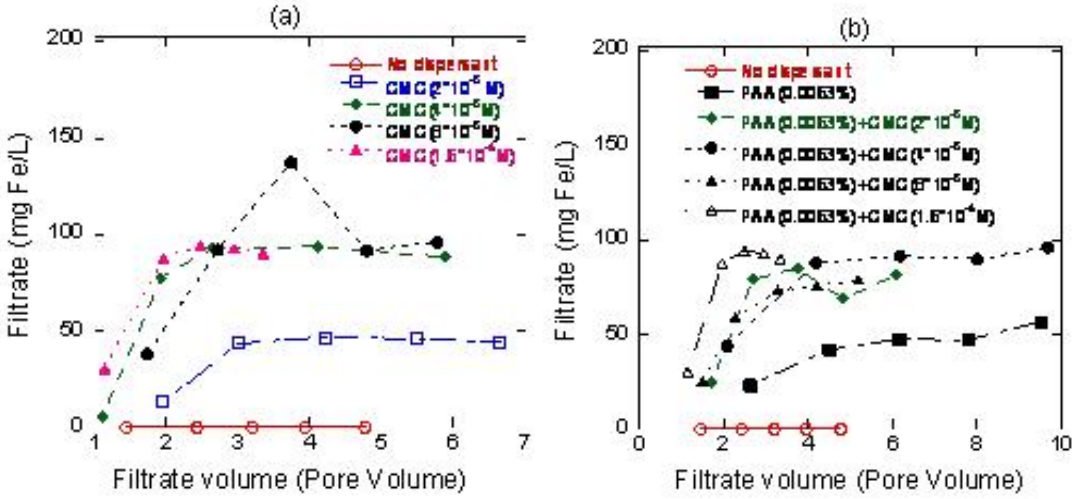

圖 3.有無 PAA 作用下，CMC 濃度對 0.1g Fe/L 零價鐵穿透石英砂層管柱之影響

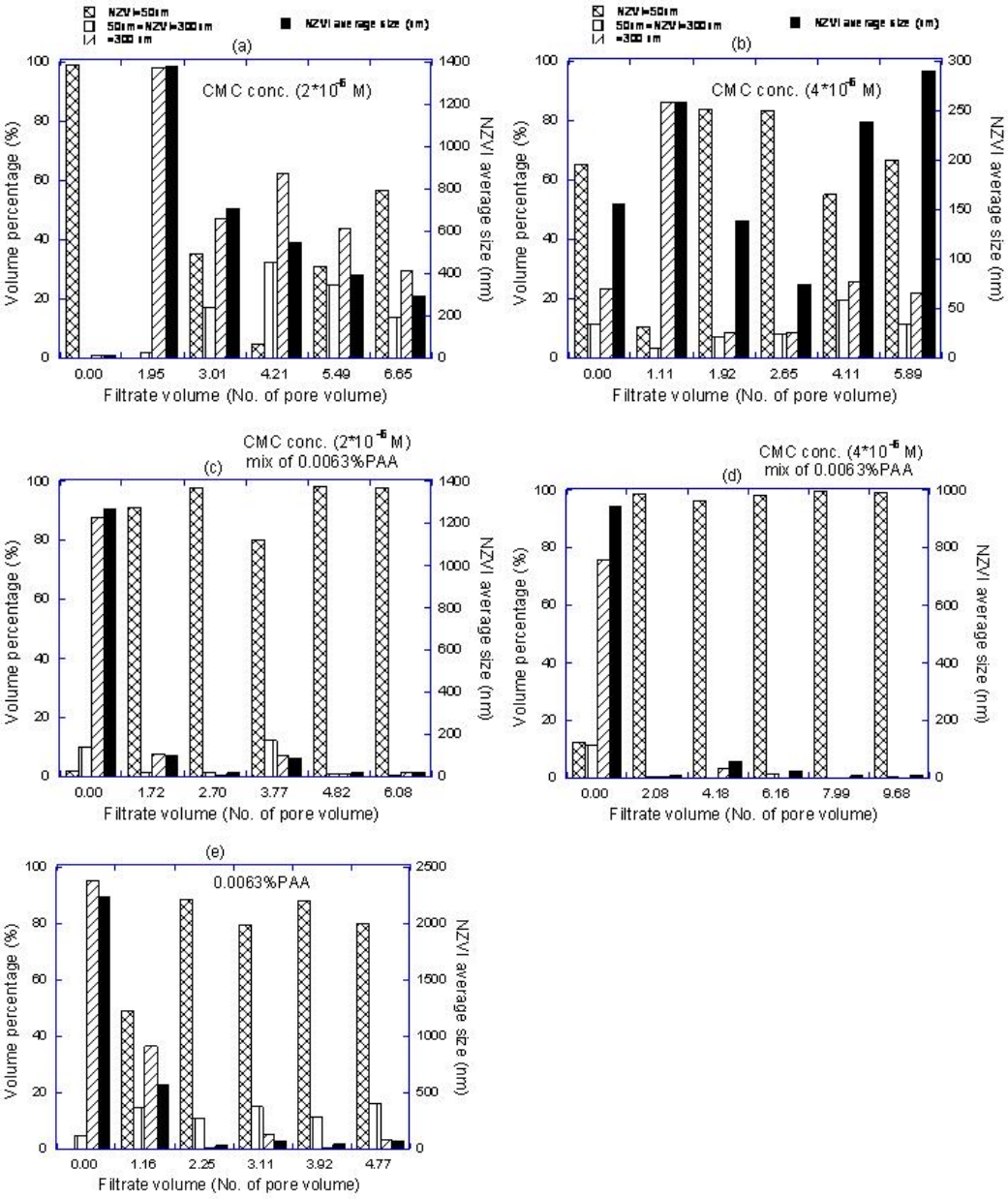

圖 4. CMC 及 PAA 對通過砂濾管柱濾出液中零價鐵分散性之影響

波長 280-430nm 之吸光值強度和雷射粒徑分析儀測量到之奈米鐵顆粒體積百分比分佈強度成正相關。以 4×10^{-6} M CMC、0.0063% PAA 和 4×10^{-6} M CMC＋0.0063% PAA 合成之零價鐵分散性較加，吸光值較高(圖 5)。

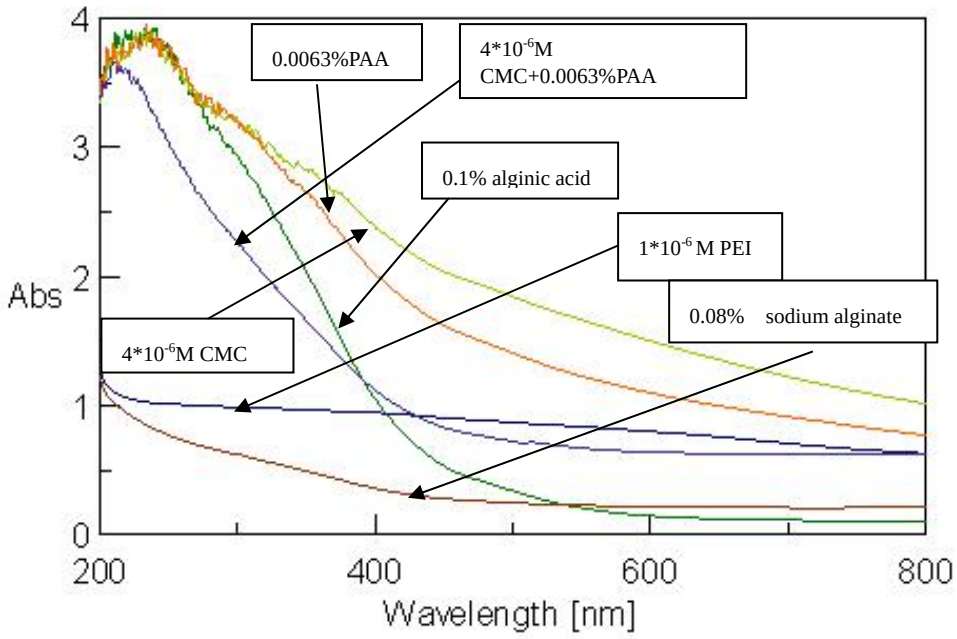

圖 5. 各種分散劑對零價鐵顆粒分散性之吸光圖譜

6. 結論與建議、

為移除地下水中含氯有機污染物、硝酸鹽、重金屬離子(如重鉻酸根離子)，零價鐵是極少數可被允許於場址現地進行注入整治之藥品，為增強零價鐵功效，降低粒徑成奈米級顆粒，增加地下孔隙間移動性成為應用上之盲點。本研究測試結果證明 CMC、PAA、PEI 等分散劑，確實可降低化學合成之零價鐵顆粒尺寸大小成奈米級，增加其在砂孔隙間之移動性。尤其使用混合式分散劑更可提高奈米級零價鐵顆粒分散性及孔隙穿透性。

承蒙國科會給予一年之應用研究補助經費，已獲致初步奈米級零價鐵顆粒穿透性及分散性成效，本研究發現混合型分散劑對提升奈米級零價鐵顆粒穿透性及分散性效果更佳。如有後續經費補助將可更專注於**混合型分散劑對提升奈米級零價鐵顆粒穿透性及分散性之研究，預期其成果將可申請專利，且馬上可應用於實際受污染場址進行整治。提高奈米級零價鐵顆粒分散性及孔隙穿透性這個主題，不只台灣有實際應用價值，全世界從事地下水汙染整治之專家學者更期盼能有突破，將使奈米級零價鐵對污染整治之貢獻更邁前一步**。

7. 計畫成果自評、

本研究內容與原計畫相符程度達 96%，完成預期工作項目及成果簡述如下

A. 找出各種分散劑對奈米級零價鐵之分散穩定效果。

Ans. 測試 SDBS、SDS、CMC、PAA、PEI、PVG、alginic acid、sodium alginate、gelatine 等對零價鐵之分散效果。

B. 找出對零價鐵之分散穩定效果最佳之分散劑濃度。

Ans. 證明 CMC、PAA、PEI、Alginic acid、及混合型分散劑之最佳穩定零價鐵顆粒濃度。

C. 找出最適宜傳送奈米級零價鐵流經多孔隙材質之分散劑。

Ans. 找到 CMC、PAA、及混合型分散劑最適宜傳送奈米級零價鐵。

D. 各種界面活性劑對奈米級零價鐵表面特性之影響

Ans.以界達電位值判斷零價鐵表面特性及其對顆粒分散性之相關性。

本研究成果極富應用價值，為目前全球地下水污染整治業界極欲找尋之克服困境方法之一，在學術上亦預期可發表於 water research 等期刊。

8. 參考文獻

1. Sun Y., Li X., Zhang W. and Wang H.P. (2007). A method for the preparation of stable dispersion of zero-valent iron nanoparticles. Colliods and Surf. A: 308, 60-66.
2. Cao J., and Zhang W. (2006). Stabilization of chromium ore processing residue (COPR) with nanoparticle iron particle. J. Hazard. Mater. B 132, 213-219.
3. Sun Y., Li X., Cao J. Zhang W. and Wang H.P.(2006). Characterization of zero-valent iron nanoparticles. Adv. Colliods and Interface Sci. 120, 47-56.
4. Schrick B., Hydutsky B.W., Blough J.L. and Mallouk T.E. (2004). Delivery vehicles for zerovalent metal nanoparticles in soil and groundwater. Chem. Mater. 16, 2187-2193.
5. Zhang Q., Thompson M.S., CarmichaeluBaranauskas A.Y., Caba B.L. Zalich M.A., Lin Y., Mefford O.T., Davis R.M., and Riffle J.S. (2007). Aqueous dispersions of magnetite nanoparticles complexed with copolyether dispersants: experiments and theory. Langmuir 23, 6927-6936.
6. Liu J., Wang L., Samuels W.D., and Exarhos G.J. (1997). Aggregation and dispersion of colloidal suspensions by inorganic surfactants: effect of chemical speciation and molecular conformation. J. Phys. Chem. B, 101, 8264-8269.
7. Kholmetskii A.L., Vorobyova S.A., Lesnikovich A.I., Mushinskii V.V. and Sobal N.S. (2005). A novel route for the preparation of magnetic fluids. Mater. Lett. 59,1993-1996.
8. Bucak S., Jones D.A., Laibinis P.E., and Hatton T.A. (2003). Protein separation using colloidal magnetic nanoparticles. Biotechnol. Prog. 19, 477-484.
9. Swartz C.H. and Gschwend P.M. (1998). Mechanisms Controlling Release of Colloids to Groundwater in a Southeastern Coastal Plain Aquifer Sand. Environ. Sci. Technol. 32, 1779-1785.
10. Lu K. (2007). Theoretical analysis of colloidal interaction energy in nanoparticle suspensions. Ceramics international. In press.
11. Zhang W. and Elliott D. W. (2006). Application of iron nanoparticles for groundwater remediation. Remediation, spring, 7-21.
12. Lien H., and Zhang W. (2007). Removal of methyl *tert*-butyl ether (MTBE) with nafion. J. Hazard. Mater. 144, 194-199.
13. Cheng R., Wang J., and Zhang W. (2007). Comparison of reductive dechlorination of *p*-chlorophenol using Fe^0 and nanoscale Fe^0. J. Hazard. Mater. B 144, 334-339.
14. Lien H., and Zhang W. (2007). Nanoscale Pd/Fe bimetallic particles: catalytic effects of palladium on hydrodechlorination. Applied Catal. B 77, 110-116.
15. Li X., and Zhang W. (2006). Iron nanoparticles: the core-shell structure and unique

properties for Ni(II) sequestration. Langmuir 22, 4638-4642.
16. Xu Y., and Zhang W. (2000). Subcolloidal Fe/Ag particles for reductive dechlogenation of chlorinated benzenes. Ind. Eng. Chem. Res. 39, 2238-2244.
17. Wang C., and Zhang W. (1997). Synthesizing nanoscale iron particles for rapid and complete dechlorination of TCE and PCBs. Environ. Sci.Technol. 31, 2154-2156.
18. Li X., and Zhang W. (2007). Sequestration of metal cations with zerovalent iron nanoparticlea-A study with high resolution X-ray photoelectron spectroscopy (HR-XPS). J Phys. Chem. C 111, 6939-6946.
19. Masciangioli T. and Zhang W. (2003). Environmental technologies at the nanoscale. Environ. Sci.Technol. 102A-108A.
20. Elliott D.W. and Zhang W. Field assessment of nanoscale bimetallic particles for groundwater treatment. Environ. Sci.Technol. 35, 4922-4926.
21. Zhang W., Wang C., and Lien H. (1998). Treatment of chlorinated organic contaminants with nanoscale bimetallic particles. Catal. Today 40, 387-395.
22. Lien H., and Zhang W. Nanoscale iron particles for complete reduction of chlorinated ethenes. Colloids Surf. A191, 97-105.
23. Ponder S.M., Darab J.G. and Mallouk T.E. (2000). Remediation of Cr(II) and Pb(II) aqueous solutions using supported, nanoscale zero-velent iron. Environ. Sci.Technol. 34, 2564-2569.
24. Choe S., Liljestrand H.M. and Khim J. (2004). Nitrate reduction by zero-valent iron under different pH regimes. Applied Geochem. 19, 335-342.
25. Source zone remediation via ZVI-clay, center for contaminant hydrology of Colorado state university, october 2004.
26. The remediation technologies development forum (http://www.rtdf.org/public/permbarr/prbsumms/default.cfm)
27. Phenrat T., Saleh N., Sirk K., Tilton R.D., and Lowry G.V. (2007). Aggregation and sedimentation of aqueous nanoscale zerovalent ion dispersant. Environ. Sci.Technol. 41, 284-290.
28. Singh B.P., Menchavez R., Takai C., Fuji M., and Takahashi M. (2005). Stability of dispersions of colloidal alumina particles in aqueous suspensions. J. Colloid Interface Sci. 291, 181－186.
29. Tufenkji N., and Elimelech M. (2004). Correlation equation for predicting single-collector efficiency in physichemical filtration in saturated porous medium. Environ. Sci.Technol. 38,529-536.

附件一

出席國際學術會議 心得報告

單　　位	嘉南藥理科技大學 環境工程與科學系	姓名	蔡利局	級職	副教授
會議名稱	第 19 屆"美國西岸土壤、底泥及水污染"研討會				
會議日期	自 98　年　3　月　9　日至　98　年　3　月　12　日				
會議地點	美國加州聖地牙哥				

會議心得

環境健康與科學協會(AEHS)每年三月份於美國西岸，南加州聖地牙哥之 Mission valley Marriott 國際飯店舉辦"西岸土壤，底泥及水污染"研討會,今年已是此類研討會之第 19 次會議(The Nineteenth Annual AEHS Meeting and West Coast Conference on Soils, Sediments, and Water)。此研討會主供國際環境科學人士、顧問公司、環境政策訂定人員、石油化學製造業及運輸業人士共同討論及交換土壤、底泥及水體中新發現之污染問題、新穎之研究技術成就、發表新穎污染防治處理技術、及據此研訂新的環境管理法規。每年吸引全球 500～600 位專門技術人員及環保官員參加，並吸引眾多重量級企業(超過 40 家)前往參展新的污染防治設備及分析方法並贊助經費，可見此研討會在北美地區受重視程度。會議期間並針對特殊專業議題舉辦 11 場 Workshops 討論會。第 19 屆研討會重點為發展創新性及低價位評估技術有助於訂定新環保法規。

個人承國科會經費補助前往美國加州聖地牙哥參加研討會並以壁報方式發表論文，題目為：Enhancement of Heavy Metals Adsorption with Chemically Modified Lignocellulosic Substrate。發表時間為 98 年 3 月 10 日下午 3 點至 6 點。當天共有 27 篇之 poster 發表，每位作者皆站在大型海報邊，供與會人士詢問疑惑及討論，個人發表之主題為利用台灣野地無適當用途之銀合歡木質部,經簡單化學修飾後提升移除水中重金屬離子之效能，亦吸引 10 幾位與會者之興趣，認為此法有助於控制外來種植物之大量繁殖，又能減少排放至水體環境之重金屬量。

除 poster 討論時間外，亦參加個人有興趣之口頭報告主題，聽取全球環保專家對土壤、水及地下水環境污染整治問題之研究心得，特別是重金屬及生物整治技術領域。此研討會把 platform(口頭報告)分成下述主題：

1. 非水溶相液體(NAPL)、
2. 重金屬(Heavy metals)、
3. 生物整治(Bioremediation)、
4. 底泥(Sediment)、
5. 場址應用臭氧整治(In-situ ozone remediation in different condition)、
6. 場址整治最適化及關閉基準(Remedy optimization and expedited

	site closure strategies with diagnostic tools)、 7. 創新整治技術(Innovative remedial technologies)、 8. 法規訂定及政策(regulatory program and policies)、 9. 水中微量醫藥物質(pharmaceuticals in water)、 10. 蒸氣逸散(vapor intrusion)、 11. MTBE/Oxygenates、 12. remediation of mining wastes、 13. Environmental forensics/legal issues、 14. Site assessment、 15. Environmental fate & modeling。 另大會議亦舉辦 11 場 Workshops 討論會，主題分別為： 1. New California luft field manual: findings from recent public meetings、 2. Perchlorate remediation technologies、 3. Environmental fate of hydrocarbon on soil and groundwater、 4. Greening the remediation industry、 5. Compound specific isotope analysis and stable isotope probing to demonstrate biodegradation of groundwater contaminants、 6. Remediation risk management: concepts and practices、 7. RBCA grows up: introduction to environmental hazard evaluation and advanced approaches for site investigations、 8. In-situ chemical oxidation: technology advances in treatment and application、 9. Geochemical evaluations of metals in environmental media: how to distinguish naturally elevated concentrations from site-related contamination、 10. Assessing vapor intrusion at petroleum release sites、and 11. Classic and emerging techniques in environmental forensics. 有幸參加此國際研討會有助於個人研究方向之修正及檢討，在目前全球經濟危機造成國家有限研究經費排擠限制下，找出符合現階段國家發展需要之實用性研究題目及能解決迫切之環境污染問題之努力方向。

附件二

出席國際學術會議發表之論文

Enhancement of Heavy Metals Adsorption with Chemically Modified Lignocellulosic Substrate

Li-jyur Tsai＊, Kuang-Chung Yu[§], Jing-song Chang＊, Muh-Yea Hung＊

＊Department of Environmental Engineering and Science, Chia-Nan University of Pharmacy and Science, Tainan 717, Taiwan, Telephone: (886) 6-2660254, Fax: (886) 6-2669090, lijyur@ms22.hinet.net.

[§]Institute of Hot Spring Industry, Chia-Nan University of Pharmacy and Science, Tainan 717, Taiwan, Telephone: (886) 6-2660017, Fax: (886) 6-2669090, kuchuyu@ksts.seed.net.tw

Abstract

The use of five chemical modification processes, including phosphorylation, sulfonation, sodium thiosulfate, citric acid and formaldehyde modification, to modify the lignocellulosic substrate of *Leucaena lucocephala* into adsorbent which could actually enhance the removal efficiency of metal ions (Cd^{2+} and Pb^{2+}) from aqueous solution. Parameters that may affect the metal ions adsorption efficiency including solution pH, contact time, kinds of metal ions, initial metal concentration, competition metal ions and reaction temperature were conducted. The best adsorption efficiencies of Cd^{2+} and Pb^{2+} with adsorbents at optimal operation condition were sequenced as phosphorylation (91.8 mg-Pb^{2+}/g, 61.2 mg-Cd^{2+}/g), sulfonation (46.2 mg-Pb^{2+}/g, 18.4 mg-Cd^{2+}/g), citric acid (43.8 mg-Pb^{2+}/g, 16.4 mg-Cd^{2+}/g), formaldehyde modification (41.0 mg-Pb^{2+}/g, 19.2 mg-Cd^{2+}/g), sodium thiosulfate (30.8 mg-Pb^{2+}/g, 12.4 mg-Cd^{2+}/g), and nonmodified adsorbents (16.8 mg-Pb^{2+}/g, 10.4 mg-Cd^{2+}/g). The adsorption capacities of Cd^{2+} and Pb^{2+} depended on solution pH. The maximum adsorbed capacity of both heavy metals happened at pH 6.5. The adsorption equilibrium reached after 60 minutes of contact time with batch kinetic studies of each metal ion and different adsorbents.

The experimental isothermal equilibrium data were evaluated with Freundlich, Langmuir, and Dubinin－Radushkevich equation isotherm models to calculate the isothermal adsorption constants and to decide the adsorption behaviour being chemical or physical reaction. Three adsorption kinetic models, Pseudo－first order rate equation, Pseudo－second order rate equation, and Intraparticle diffusion equation, were used to evaluate the experimental data. Under the effects of reaction temperature, initial metal concentration and competition metal ions, pseudo－second order rate equation model best fitted to experimental data. The thermodynamic parameters (enthalpy change, free energy change, and entropy change) for both metal ions adsorption into six adsorbents with increasing temperature from 15 to 60 ℃ indicated that the Pb^{2+} adsorption was exothermic and feasible, and the Cd^{2+} adsorption was endothermic and feasible. The competition of binary heavy metal ions into six kinds of adsorbents also studied. The binding strength of Pb^{2+} was stronger than Cd^{2+} and increased with the initial heavy metal ions concentration.

Keywords：Lignocellulosic substrate, Heavy metal, Adsorbent, phosphorylation, kinetic adsorption models.

1. Introduction

White Popinac (Leucaena lucocephala), a small-diameter underutilized wood material, an exotic plant has caused devastating damages on native plants of southern Taiwan. Five chemical modification processes, including phosphorylation, sulfonation, sodium thiosulfate, citric acid and formaldehyde modification, modified the sawdust material (wood of White Popinac, primarily containing lignocellulosic substrate) into adsorbent which could be actually enhanced the removal efficiency of metal ions (Cd^{2+} and Pb^{2+}) from aqueous solution. The considered parameters affecting metal ions adsorption were contact time, initial pH, reaction temperature, initial metal concentration, and adsorbent dosages. Three adsorption kinetic models including pseudo-first-order, pseudo-second-order, and intraparticle diffusion equations were used to discuss the adsorption mechanism of Lead (II), and Cadmium (II) ions onto adsorbents.

2. Material and methods

2.1. Adsorbent

The lignocellulosic substrate of *Leucaena lucocephala* collecteded from a wild field in Tainan county, Taiwan, was grounded, sieved into 30-40 mesh particles and dried at 70 ℃ used in the adsorption process. Preparation of chemically modified lignocellulosic substrate was carried out with chemically modification treatments, consisting of phosphorylation, sulfonation, sodium thiosulfate, citric acid or formaldehyde modification. The modification procedure was described below. Also the 30-40 mesh particles were collected for the adsorption process after the modification process.

2.2. Type of modification：

2.2.1. phosphorylation (Klimmek et. al., 2001)

Mixture of 300 gram lignocellulosic substrate and 450 gram urea was added into 500 mL 30% of phosphoric acid. The mixture was stirred, stayed in room temperature for 30 min and stored at 70℃ oven to distill the water till slurry formed. The lignocellulosic substrate mixture was allowed to cool and washed with deionized water to remove the residual chemicals. The modified lignocellulosic substrate was dried at 150 ℃ for 24 hours and then ground to 30-40 mesh for adsorption test.

2.2.2. sulfonation (Shin et. al., 2005)

20 gram lignocellulosic substrate and 25.2 gram Sodium sulfite was mixed into 300 mL water. The pH of wet lignocellulosic substrate was adjusted to 3.0 with 1.0 N nitric acid. The wet lignocellulosic substrate proceeded sulfination for 1 day at 70℃. The treated

lignocellulosic substrate was centrifugated at 9,000 g for 10 minutes and washed with distilled water at least three times to remove residual chemicals and then dried at 70 ℃ oven.

2.2.3. Citric acid modification (Marshall et. al., 1999)

One thousand grams of lignocellulosic substrate were placed in a 10 L beaker and mixed with approximately 5000 mL of 0.1 N NaOH at room temperature. The mixture was stirred for 60 minutes and then the liquid was discarded. The wet lignocellulosic substrate was washed with deionized water until the pH value decreased to 8.0. After that 1000 ml of 0.6 M citric acid was mixed with lignocellulosic substrate pretreated with NaOH and dried over night at 50 ℃ in a forced air oven, after that the temperature was raised to 100 ℃ and hold there for 8 hours. The lignocellulosic substrate was allowed to cool and washed with deionized water until the pH of effluent reach at 7.0. The modified lignocellulosic substrate was dried at 70 ℃ for 24 hours and then destroyed with grinder and stored for adsorption test.

2.2.4. Sodium thiosulfate modification (Xie et al., 1996)

For modification using $Na_2S_2O_3$, 1000 g of lignocellulosic substrate was treated with 200 g $Na_2S_2O_3$ in 600 mL deionized water at 90℃ for 12 hours. The treated lignocellulosic substrate was pelleted by centrifugation at 9,000 g for 10 minutes and washed with distilled water at least three times, and then dried in 90℃ oven. Sodium thiosulfate yields adsorbent with additional sulfhydryl groups resulting improvement in metal-binding capacity. The modified lignocellulosic substrate was then destroyed with grinder and stored for adsorption test.

2.2.5. Formaldehyde modification (Palma et al, 2003):

One thousand grams of 30-40 mesh lignocellulosic substrate was mixed with 3000 mL 10% nitric acid and 25 mL 37% formaldehyde solution in a 5 L beaker. The mixture was stirred and stored at 80℃ oven for 1 hour. The lignocellulosic substrate mixture was allowed to cool and washed with deionized water to remove the residual chemicals. The modified barley waste was dried at 50 ℃ for 24 hours and then ground to 30-40 mesh for adsorption test. This modified lignocellulosic substrate was called 0.25 mL formaldehyde modified adsorbent. Similarly, the used dosage of 37% formaldehyde solution changed into 100 mL, the obtained adsorbent was called 1.0 mL formaldehyde modified adsorbent.

2.3. Reagents and solutions

Cadmium and Lead ion stock solutions (1 mg/mL) were prepared by dissolving 137.215 g of $Cd(NO_3)_2$, and 79.956 g of $Pb(NO_3)_2$ (Merck), respectively into 5L deionized water. Working solution of the Cd^{2+}, Pb^{2+} ions were prepared by suitable dilution of the stock solution with deionized water into 25, 50, 100, 150, 200, 300, 500, 1000, and 1500 mg/L for further

experimental solution preparation. Before mixing the adsorbents, the pH of each test solution was adjusted to the required value with 0.1 M nitric acid or 0.1 M sodium hydroxide. The concentration of Cd^{2+}, and Pb^{2+} ions in the stock solutions and remaining in the filtrate was determined with atomic absorption spectrometry at 228.8 and 283.8 nm, respectively (GBC model 932, Australia).

2.4. Isothermal adsorption experiment

For Cd^{2+} ions sorption studies, 0.25 g adsorbent brought into contact with 100 mL of Cd^{2+} solution at constant speed (150 rpm) at 30℃ using orbital thermostatic shaker for 2 hours, this operation time was considered sufficient to reach adsorption equilibration. After filtration, the residual concentration of Cd^{2+} in the filtrate was analyzed with atomic absorption spectrometry. The adsorption capacity of Cd^{2+} ions by adsorbent was calculated with the difference of initial and final Cd^{2+} concentration in aqueous solution. The adsorption capacity of Cd^{2+} ions adsorbed per gram adsorbent (mg/g) was calculated using

$$Q=[(C_o-C_t)\times V]\div W$$

where C_o and C_t are the initial and at any time (t) concentration (mmol /L) of Cd^{2+} in the solution, V the volume (L) of solution and W is the weight (g) of the adsorbent.

The effect of hydrogen ion on competitive adsorption of Cd^{2+} ions was evaluated by adjusting the initial pH of contact solution over the range of approximately 2-8. The pH of initial solution was adjusted to the pH value using 0.1 M nitric acid or sodium hydroxide.

Three adsorption isothermal models were used to express the mathematical relationship between the quantity of adsorbed Cd^{2+} ions and the equilibrium concentration of Cd^{2+} ions remaining in the solution at a constant temperature, which are Langmuir (Heimenz, 1986), Freundlich (Kinniburgh, 1986) and Dubinin-Radushkevich(D-R) equations (Dubinin & Radushkevich, 1947).

2.4.1. Langmuir isotherm model

Langmuir adsorption isotherm assumes that the uptake of solute occur on a homogenous surface by monolayer adsorption without any interaction between adsorbed ions and interfered with other ions in solution. The Langmuir equation may be written as the following linear form

$$1/Q_e = 1/Q_{max} + 1/(Q_{max} \times K_L \times C_e)$$

For the equilibrium conditions in these equations, C_e and Q_e are the concentration of metal ions (mmol/L) in solution and metal ions adsorbed to per unit mass of adsorbent (mmol/g) at equilibrium. The constant K_L related to the affinity of binding sites or bonding energy with unit of (L/mg). The constant Q_{max} is the maximum adsorption capacity of adsorbent and has the unit of (mmol/g). A plot of $1/Q_e$ versus C_e should be a straight line with a slope $1/(Q_{max} \times K_L)$ and intercepts $1/Q_{max}$. The essential characteristic of Langmuir isotherm can be explained in dimensionless constant called separation factor R_L, which is defined as the following relationship (Webi & Chakravort, 1974):

$$R_L=1/(1+K_L\times C_o)$$

where K_L and C_o are Langmuir constant and initial concentration of solute in solution. The value of R_L can indicate the shape of isotherm whether an adsorption system is linear irreversible (R_L=0), favorable (0<R_L<1), linear (R_L=1), or unfavorable (R_L>1).

2.4.2. Freundlich isotherm model

Freundlich adsorption isotherm assumes that the uptake of solute occur on a heterogeneous surface by multilayer adsorption. The Freundlich equation may be written to the following linear form as (Webi & Chakravort, 1974):

$$\ln Q_e = \ln K_F + 1/n \times \ln C_e$$

where Q_e is the amount of solute adsorbed per unit weight of adsorbent (mmol/g), C_e is the solute concentration in solution at equilibrium (mmol/L). K_F is constant of Freundlich isotherm incorporating adsorption capacity (mmol/g) and n is the adsorption intensity.

2.4.3. Dubinin-Radushkevich(D-R) isotherm model

The Dubinin-Radushkevich(D-R) isotherm equation is more general than the Langmuir and the Freundlich isotherm models because it does not assume a homogeneous surface or constant adsorption potential (Unlu and Eraoz, 2006). D-R equation can be used to distinguish between physical and chemical adsorption of Cd^{2+} ion. The linear form of D-R equation is (Dubinin and Radushkevich, 1947):

$$\ln Q_d = \ln Q_m - \beta \times \varepsilon_e^2$$

$$\varepsilon_e \text{ (Polanyi potential)} = RT \times \ln(1+(1/C_f))$$

where Q_d (mol/g) and Q_m (mol/g) are the amount of solute adsorbed per unit weight of adsorbent and the maximum adsorption capacity. β (mol^2kJ^{-2}) is a constant related to the adsorption energy. C_f is the equilibrium Cd^{2+} ion concentration in the solution (mol/L). When the solute in the solution is transferred to the surface of the adsorbate solid from infinity, the adsorption energy for per molecule of the adsorbate is defined as mean free energy E ($kJmol^{-1}$) and expressed as:

$$E = 1/(2\beta)^{0.5}$$

The E value is useful for the estimation of adsorption process type. The adsorption process adjusted to chemical ion-exchange when the magnitude of E is between 8 and 16 $kJmol^{-1}$. The adsorption process adjusted to physical nature when the magnitude of E lower than 8 $kJmol^{-1}$(Onyango et al., 2004).

2.5. Adsorption kinetic parameters

0.25 g of chemically modified lignocellulosic substrate was added to 100 mL of Cd^{2+} ions solution in 150 ml Erlenmeyer flasks. By adding small amounts of HNO_3 or NaOH solution, the initial pH of the solution was adjusted to the optimal value of each adsorbent. The flasks were placed in an orbital thermostatic shaker bath with 15℃, 30℃, 50℃, or 70 ℃ at 150 rpm for various time intervals (0, 5, 15, 30, 60, and 120 minutes). At the end

of a specified time period, the flasks were removed and the Cd^{2+} ion remaining in the solution was analyzed. Various kinetic models including the pseudo-first order rate equation, pseudo-second order rate equation, and intraparticle diffusion equation have been applied for the experimental data to predict the adsorption kinetics.

2.5.1. pseudo-first order rate equation

A linear form of the pseudo-first order rate equation is (Ho, Y.S. and McKay G., 1998a, b):

$$1/q_t = 1/q_1 + k_1/(q_1 \times t)$$

where q_1 (mg/g) and q_t (mg/g) are the amounts of the Cd^{2+} ions adsorbed at equilibrium and at time t and the k_1 (min^{-1}) is the pseudo-first order rate constant of adsorption.

2.5.2. pseudo-second order rate equation

A linear form of the pseudo-second order rate equation is (Ho, Y.S. and McKay G., 1998a):

$$t/q_t = 1/(k_2 \times q_2^2) + t/q_2$$

where q_2 (mg/g) and q_t (mg/g) are the amounts of the Cd^{2+} ions adsorbed at equilibrium and at time t and the k_2 (min^{-1}) is the pseudo-second order rate constant of adsorption.

2.5.3. Intraparticle diffusion equation

A linear form of the intraparticle diffusion equation is (Weber and Morriss, 1963):

$$q_t = C + k_p \times t^{0.5}$$

where k_p is the intraparticle diffusion rate constant at time t and the value of C get from the intercept.

2.6. Thermodynamic parameters of adsorption

The thermodynamic parameters such as Gibbs free energy change (ΔG^0), enthalpy change (ΔH^0), and entropy change (ΔS^0) could be used to describe the spontaneous and heat change of the adsorption process (Eligwe et al., 1999). The apparent equilibrium constant (K_c) (mg/mL) of the Cd^{2+} ion adsorption is defined as (Akzu and Isoglu, 2005; Malkoc and Nuhoglu, 2005):

$$K_c = C_{ad,eq} \div C_{eq}$$

where $C_{ad,eq}$ (mg/g) and C_{eq} (mg/mL) are the Cd^{2+} ion concentration adsorbed on the adsorbent and residual in the filtrate solution after equilibrium.

The Gibbs free energy change in the adsorption reaction is given by the following equation:

$$\Delta G^0 = -RT \times \ln K_c$$

where R (8.314 $Jmol^{-1}K^{-1}$) is the ideal gas constant and T (°K) is the absolute temperature. The Gibbs free energy also can be represented in the linear form as:

$$\ln K_c = -\Delta H^0 \div (RT) + \Delta S^0 \div R$$

The enthalpy change (ΔH^0) and entropy change (ΔS^0) were determined from the slope and

intercept of the linear plot between $\ln K_c$ versus 1/T.

Similarly, the isothermal adsorption experiments, adsorption kinetic parameters, and thermodynamic parameters of adsorption were carried out with Pb^{2+} ions onto chemically modified lignocellulosic substrate.

3. Results and discussion

3.1 Adsorption isotherms

To realize the equilibrium adsorption capacities of Cd^{2+} and Pb^{2+} by adsorbents modified from lignocellulosic substrate with phosphorylation, sulfonation, sodium thiosulfate, citric acid and formaldehyde modification, different concentration of Cd^{2+}, and Pb^{2+} (25, 50, 100, 200, 500, 1000, and 1500mg/L) was used to test. The adsorbed heavy metals per gram adsorbent increased with heavy metals concentration in aqueous solution until isothermal equilibrium adsorption reached (figures 1, 2). The enhancement of equilibrium adsorption capacity of Pb^{2+} with chemically modified lignocellulosic substrate ordered as phosphorylation, sulfonation, citric acid, formaldehyde, sodium thiosulfate and lignocellulosic substrate without modification. Similarly, the chemically modification also enhanced the Pb^{2+} adsorption onto lignocellulosic substrate. The adsorption capacity of Pb^{2+} was in the order of phosphorylation, formaldehyde, sulfonation, citric acid, sodium thiosulfate and lignocellulosic substrate without modification.

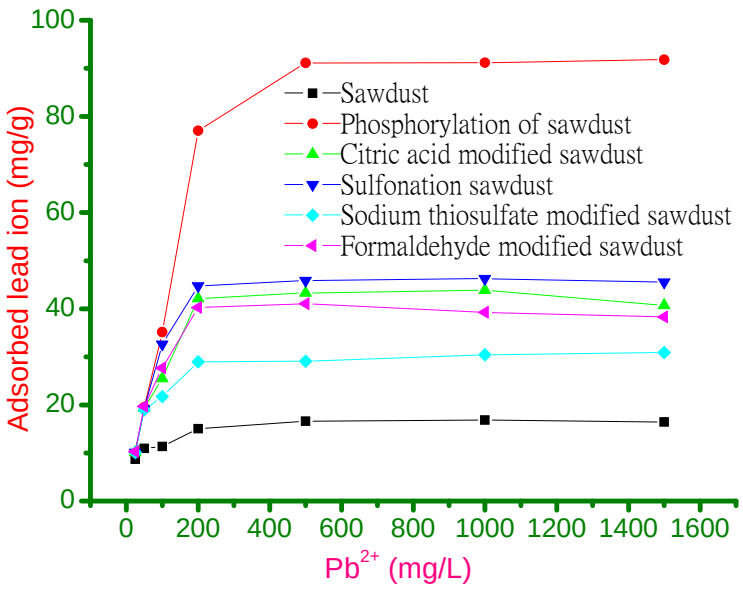

Figure1. Isotherm adsorption of Pb^{2+} onto various adsorbents. Operation condition: 2 g adsorbent mixed with 800 mL Pb^{2+} solution at 800 rpm, pH 6.1～6.5 and 30℃.

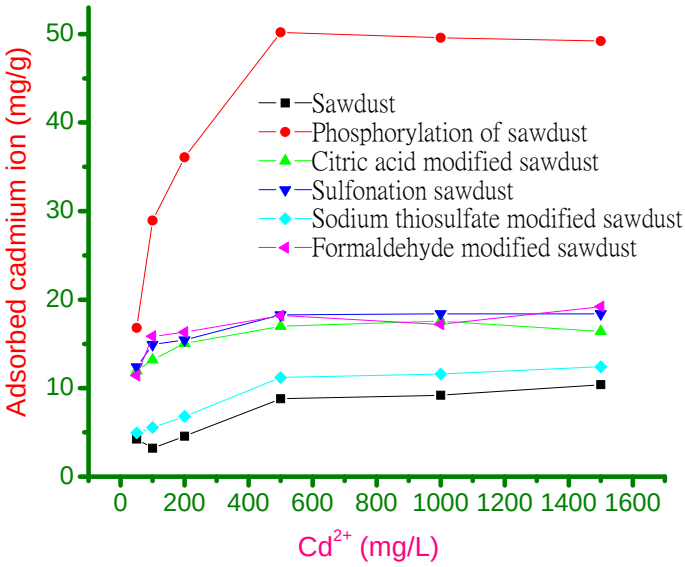

Figure2. Isotherm adsorption of Cd^{2+} onto various adsorbents at 30℃. Operation condition: 2 g adsorbent mixed with 800 mL Cd^{2+} solution at 800 rpm, pH 6.1～6.5 and 30℃.

Three isotherm adsorption models (Freundlich equation, Langmuir equation, and Dubinin-Radushkevich equation) (Brenhammou et al., 2005) were used to predict the interaction of Cd^{2+} and Pb^{2+} ions with lignocellulosic substrate adsorbents modified with chemicals. The experimental data of Cd^{2+} and Pb^{2+} ions adsorbed onto the adsorbents at equilibrium can be used to calculate and evaluate the characteristics of isothermal equilibrium adsorption. The adsorption capacity fitness of Cd^{2+} and Pb^{2+} ions onto adsorbents was calculated and predicted from experimental data by three isothermal adsorption models as shown in Table 1.

The mean free energy E ($mol^{-1}kJ$) of Cd^{2+} and Pb^{2+} ions adsorption calculated from D-R equation was listed in Table 1. The magnitude of E was between 9.3 and 24.9 $mol^{-1}kJ$ and meant that the adsorption mechanism between Cd^{2+} and Pb^{2+} ions and adsorbents belong to chemical ion-exchange process. If E values smaller than 8 $mol^{-1}kJ$, the adsorption process was thought as physical nature (Onyango et. al., 2004). The adsorption of Cd^{2+} and Pb^{2+} ions by adsorbent modified with phosphorylation, sulfonation, citric acid, formaldehyde, and sodium thiosulfate was chemical ions exchange reactions (Table 1).The adsorbents from phosphorylation, sulfonation, citric acid, formaldehyde, and sodium thiosulfate had Pb^{2+} ion adsorption behavior which could be predicted with Langmuir model in high correlation coefficient (r_L^2) 0.95, 0.97, 0.97, 0.97 and 0.97, respectively. For adsorption of Cd^{2+} ion with adsorbents modified from phosphorylation, sulfonation, citric acid, formaldehyde, and sodium thiosulfate, the adsorption behavior fitted the Freundlich model better than Langmuir model with higher correlation coefficient (r_L^2) 0.99, 0.98, 0.94, 0.98 and 0.93, respectively.

Table 1 Coefficients of Determination for Isothermal Adsorption Models

Metals	Adsorbents	Freundlich Eq.	Langmuir Eq.	Free energy (KJ/mol)
Pb^{2+}	Sawdust	0.94∨	0.74	20.4
	Phosphorelation of sawdust	0.73	0.95∨	15.2
	Citric acid modification	0.87	0.97∨	17.8
	Sulfonation sawdust	0.82	0.97∨	17.7
	Sodium thiosulfate modification	0.87	0.97∨	20.9
	Formaldehyde modification	0.86	0.97∨	20.3
Cd^{2+}	Sawdust	0.81	0.99∨	9.3
	Phosphorelation of sawdust	0.99∨	0.88	16.7
	Citric acid modification	0.94∨	0.77	22.8
	Sulfonation sawdust	0.98∨	0.75	24.9
	Sodium thiosulfate modification	0.93∨	0.69	12.7
	Formaldehyde modification	0.98∨	0.87	20.3

3.2 Effect of pH

The adsorbed capacities of Cd^{2+} and Pb^{2+} onto adsorbents increased gradually from solution pH 2.0 to 6.5 (shown as figure 3 and 4). The maximum adsorbed capacity of both heavy metals (Cd^{2+} and Pb^{2+}) appeared near pH 6.5. The largest increased adsorption capacity of Cd^{2+} and Pb^{2+}) with increase of solution pH value was adsorbent modified with phosphorylation.

3.3 Adsorption kinetics

To determine the order of the heavy metal ions adsorption kinetics, pseudo-first order rate, pseudo-second order rate and intraparticle diffution equation were tested to fit the experimental data. The chemically modification methods were useful for the enhancement of adsorption capacity of Pb^{2+} and Cd^{2+} ions onto the adsorbents than lignocellulosic substrate without modification. The q_2 values calculated from pseudo-second order equation can be used to certificate this result (Table 2).

The Pb^{2+} and Cd^{2+} ions experimental adsorption data onto five chemically modified sawdust adsorbents fitted well to the pseudo-second order equation, and provided the best

description of the data with a correlation coefficient (r^2) almost near 1.0 at pH range of 6.1-6.5.

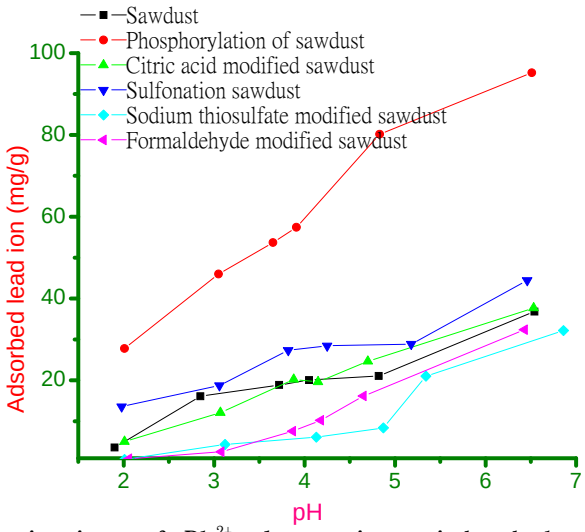

Figure 3. Variation of Pb^{2+} adsorption with ph by various adsorbents.

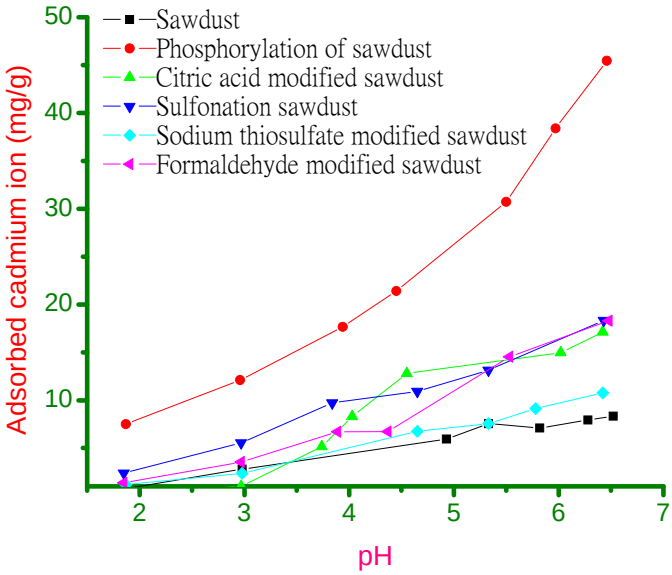

Figure 4. Variation of Cd^{2+} adsorption with ph by various adsorbents.

3.4 Thermodynamic parameter

Table 3 summarized the values of thermodynamic parameters ΔG^0, ΔH^0, and ΔS^0 for Pb^{2+} ion adsorption controlled isothermally from 15℃、30℃、45℃、to 60℃ onto adsorbents modified with phosphorylation, sulfonation, citric acid, formaldehyde, and sodium thiosulfate. The values of ΔG^0 were all negative for Pb^{2+} ion adsorption using raw and chemically modified barley waste at working temperature from 15℃ to 60℃. The absolute value of ΔG^0 increased with the increase of adsorption temperature regardless the nature of adsorbents indicated that adsorption process is spontaneously endothermic reaction and the apparent equilibrium constants (K_c) were larger than zero. The negative value of ΔH^0

coincided with the exothermic reaction process. The positive values of ΔS^0 suggested the increase of randomness at the interactive interface of adsorbent solid and Pb^{2+} ion in solution and also indicated that the adsorption reaction is spontaneous at general ambient environment.

Table 2 Comparison of parameters derived from adsorption kinetics models

Metals	Chemicals	Pseudo-first order Eq.			Pseudo second-order Eq.			Intraparticle diffution Eq.		
		q_1 (mg/g)	k_1 (1/min)	r_1^2	q_2 (mg/g)	k_2 (g/mg.min)	r_2^2	c (mg/g)	kp (mg/g.min$^{1/2}$)	r_p^2
Pb^{2+}	None	11.03	0.214	0.72	11.68	0.027	1.00	10.10	0.056	0.64
	Phosphorelation	35.34	0.131	0.96	35.59	0.049	1.00	34.10	0.056	0.23
	Citric acid	26.25	0.055	0.31	25.32	-0.022	1.00	26.34	-0.025	0.13
	Sulfonation	32.05	0.343	0.96	32.47	0.072	1.00	29.17	0.136	0.31
	Thiosulfate	24.21	0.847	0.97	25.25	0.020	1.00	19.85	0.213	0.39
	Formaldehyde	28.82	-0.086	0.16	26.04	-0.006	1.00	31.17	-0.160	0.84
Cd^{2+}	None	3.45	0.314	0.48	4.382	0.011	1.00	2.87	0.042	0.94
	Phosphorelation	27.17	0.399	0.78	29.59	0.006	1.00	23.61	0.208	0.58
	Citric acid	12.33	-0.101	0.78	12.48	0.073	1.00	12.69	-0.013	0.09
	Sulfonation	14.35	0.096	0.63	14.88	0.015	1.00	12.84	0.028	0.36
	Thiosulfate	4.82	0.689	0.84	5.79	0.011	1.00	3.82	0.062	0.71
	Formaldehyde	15.13	-0.109	0.72	15.08	0.224	1.00	15.73	-0.029	0.24

4. Conclusion

The Langmuir adsorption isotherm model was better than Freundlich equation to describe the adsorption behaviour of Pb^{2+} ions onto chemically modified adsorbents. Inversely, for the adsorption of Cd^{2+} the fitness of Freundlich isothermal adsorption model was better than Langmuir adsorption isothermal model. The ΔG^0 values were all negative for Pb^{2+} ion adsorption onto chemically modified sawdust at contacting temperature from 15℃ to 60 ℃. Similar thermodynamic characteristics also were found for Cd^{2+} ion onto modified lignocellulosic substrate. The negative value of ΔH^0 coincided with the exothermic adsorption of Pb^{2+} ion. However, the adsorption of Cd^{2+} ion was endothermic reaction. The positive values of ΔS^0 suggested the increase of randomness between surface active site of adsorbent and Pb^{2+}, Cd^{2+} ions in solution and also indicated that the adsorption reaction is spontaneous at ambient environment.

Table 3 Thermal dynamic adsorption parameters of Lead ion onto various adsorbents

Adsorbents	T (℃)	ΔG° (KJ/mole)	ΔH° (KJ/mole)	ΔS° (KJ/mole-K)	r^2
Sawdust	15	-12.934	-1.1526	0.0402	0.93
	30	-13.025			
	45	-13.986			
	60	-14.626			
Phosphorelation of sawdust	15	-25.382	-2.0215	0.08	0.91
	30	-25.591			
	45	-27.808			
	60	-28.642			
Citric acid modification	15	-16.989	-7.7136	0.0324	0.94
	30	-17.711			
	45	-17.816			
	60	-18.573			
Sulfonation sawdust	15	-19.699	-7.6801	0.0424	
	30	-20.792			
	45	-21.255	0.94		
	60	-21.666			
Sodium thiosulfate modification	15	-14.837	-6.3367	0.0299	
	30	-15.557			
	45	-15.794	0.96		
	60	-16.251			
Formaldehyde modification	15	-18.697	-2.0273	0.0581	
	30	-19.598			
	45	-20.790	0.97		
	60	-21.206			

5. References

Akzu Z. and Isoglu I. A., (2005). Removal of copper ions from aqueous solution by biosorption onto agricultural waste sugar beet pulp, Process Biochem. 40, 3031-3044.

Brenhammou A., Yaacoubi A., Nibou L., Tanouti B. (2005). Adsorption of metal ions onto Moroccan stevensite: kinetic and isotherm studies, J. Colloid Interface Sci. 282(2), 320-326.

Dubinin M.M. and Radushkevich, L.V., (1947). Proc. Acad. Sci. U.S.S.R. Phys. Chem. Sect. 55, 331.

Eligwe C.A., Okolue N.B., Nwambu C.O., Nwoko C.I.A., (1999). Adsorption thermodynamics and kinetics of mercury(II), cadmium(II), and lead(II) on lignite. Chem. Eng. Technol. 22(1), 45-49.

Heimenz P.C. (1986). Priciples of colloid and surface chemistry. 2nd. Marcel Dekker, N.Y.

Ho Y.S., McKay G., (1998a). The kinetics of sorption of basic dyes from aqueous solution by sphagnum moss peat. Can. J. Chem. Eng.76(4), 822-827.

Ho Y.S., McKay G., (1998b). Kinetic models for the sorption of dyes from aqueous solution by wood. J. Environ. Sci. Health Part B: Process Saf. Environ. Prot. 76(B2), 183-191.

Kinniburgh D.G. (1986). "General purpose adsorption isotherms". Environment Science and Technology 20, 895-904.

Klimmek, K.S., H.J. Stan, A. Wilke, G. Bunke, R. Buchholz, Comparative analysis of the biosorption of cadmium, lead, nickel, and zinc by algae. Environmental Science and Technology 35(21): 4283-4288, 2001.

Marshall, W.E., L.H. Wartelle, D.E. Boler, M.M. Johns, and C.A. Toles, Enhanced metal adsorption by soybean hulls modified with citric acid. Bioresource Technology 69(3): 263-268, 1999.

Onyango M.S., Kojima Y., Aoyi O., Bernardo E.C. Matsuda H., (2004). Adsorption equilibrium modeling and solution chemistry dependence of fluoride removal from water by trivalent-cation-exchanged zeolite F-9. J. Colloid Interface Sci. 279(2), 341-350.

Palma G., Freer J. and Baeza J. (2003). Removal of metal ions by modified *Pinus radiate* bark and tannins from water solutions. Water Research 37, 4974-4980.

Shin, E.W., and R.M. Rowell, Cadmium ion sorption onto lignocellulosic biosorbent modified by sulfonation: the origin of sorption capacity improvement. Chemosphere 60: 1054-1061, 2005.

Unlu, N. and Eraoz, M. 2006. Adsorption characteristics of heavy metal ions onto a low cost biopolymeric sorbent from aqueous solutions. J. Hazard. Mater. B136, 272-280.

Weber W. J. Jr. and Morriss J.C., (1963). Kinetics of adsorption on carbon from solution. J. Sanitary Eng. Div. Am. Soc. Civ. Eng. 89, 31-60.

Webi T.W.and Chakravort,R.K. (1974). Pore and solid diffusion models for fixed-bed adsorbers. J. AM. Inst Chem. Eng. 20(2), 228-238.

Xie, J.Z., H-L. Chang, and J.J. Kilbane, Removal and recovery of metal ions from wastewater using biosorbents and chemically modified biosorbents. Bioresource Technology 57(2): 127-136, 1996.